International Journal of Microwave and Wireless Technologies, 2018, 10(4), 446–452.
doi:10.1017/S1759078717001337

RESEARCH PAPER

1D and 2D phase gradient perforated dielectric reflective surfaces at *mm*Wave

MUSTAFA K. TAHER AL-NUAIMI[1], WEI HONG[1] AND XIQI GAO[2]

This paper presents the design of all dielectric non-absorptive phase gradient reflective surfaces that can be used to manipulate the reflected electromagnetic waves at millimeter-wave regime. Compared with a bare perfect electrical conductor reflector which obeys the classical Snell's law of reflection, the presented design can effectively alter both the shape and level of the back-scattered energy and thus radar cross section (RCS) reduction is achieved in the specular direction. One- and two-dimensional phase gradient reflective dielectric surfaces of phase change about 72° across their apertures are designed and their ability to manipulate the reflected waves under normal incidence are investigated both by means of full-wave simulations and experimentally tested for validation. More than 6 dB of specular RCS reduction is achieved from about 66.5–78.2 GHz.

Keywords: Reflection, Phase gradient, Radar cross section

Received 23 July 2017; Revised 1 November 2017; Accepted 9 November 2017; first published online 14 December 2017

I. INTRODUCTION

Manipulation of refractive and reflective electromagnetic (EM) waves have been a topic of interest in the last decade [1, 2] for many applications such as surface wave couplers [2], high gain lens antennas [3], radar cross-section (RCS) reduction [4], focusing metasurface [5], beam splitter [6]... etc. Phase gradient surface (PGS) [7, 8] is a class of engineered surfaces that consist of an array of resonators (inclusions or unit cells) and can be designed based on the concept of phase discontinuities (the generalized law of reflection) [1] to have phase discontinuity (phase change or phase jumps or phase variation) across the PGS aperture. Using PGS, the wave front of the reflected/refracted waves can be controlled more freely by using unit cells (resonators) of varying phase response. Hence, PGS can realize (for instance) negative refraction or reflection, surface wave conversion, anomalous refraction and reflection, and so on. Unit cells of various geometrical shapes can be used to compose the PGS, for example, split ring resonator [9], I-shaped [10]... etc. In [3] a multi-layer phase gradient metasurface was employed to design an X-band high gain transmitarray lens antenna which is engineered to focus the incident EM plane wave to a point with high gain. In [3] the phase-gradient unit cell having four metallic layers and three intermediate dielectric layers. Each metallic layer consists of a solid circle patch inside and a square ring outside. In [2] a specific PGC was proposed to convert the propagating waves into surface waves using metallic "'H" like resonators. In [6] a two-dimensional (2D) beam splitter tri-layer transmissive phase gradient metasurface was designed based on the generalized Snell's law of refraction. The super unit cell used consists of 6×6 unit cells with 60° phase gradient in y-direction and $-60°$ phase gradient in x-direction, respectively. The unit cell is composed of two intermediate dielectric layers and three metallic layers.

This paper presents the design of 1D and 2D non-absorptive all dielectric phase gradient perforated reflective surfaces that can be used to manipulate the shape and level of the backscattered RCS pattern and reducing the monostatic RCS of a metallic sheet. The proposed Surfaces are designed at millimeter-wave frequencies as this frequency band (60–80 GHz) is expected to be used in several future communication systems. The design is totally based on the free space wavelength and the surface can be designed at any desired frequency. The surfaces are investigated both numerically and experimentally at millimeter-wave regime.

II. THEORY OF PGSs

When there are constant phase changes (phase jumps) along with an interface between free space and a surface then an anomalous reflection would occur and can be described by the generalized law of reflection [1]. Based on this principle a surface with certain phase jumps (phase change or phase gradient) across its aperture and along the air–surface interface can manipulate the reflected energy (amplitude and phase). In 1D phase gradient reflective surface the phase change is either along x- or y-axis and can be denoted as $\Delta\phi/\Delta x$ or $\Delta\phi/\Delta y$. In case of a surface that consists of a number of periodic unit cells, the relation between the phase change along the interface ($\Delta\phi/\Delta x$) and the reflected wave amplitude/phase can be derived starting from the generalized

[1]State Key Laboratory of Millimeter waves, School of Information Science and Engineering, Southeast University, Nanjing 210096, People's Republic of China
[2]National Mobile Communications Research Laboratory, Southeast University, Nanjing 210096, People's Republic of China
Corresponding author:
M. K. T. Al-Nuaimi
Email: mustafa.engineer@yahoo.com

Snell's law of reflection [1] as in equation (1).

$$\sin(\theta_r) - \sin(\theta_i) = \frac{1}{n_i k_o}\frac{\Delta\varphi}{\Delta x} = \frac{\lambda_o}{2\pi}\frac{\Delta\varphi}{\Delta x}, \quad (1)$$

where λ_o is the free space wavelength of the incident EM waves, θ_r and θ_i are the angles of reflection and incidence, respectively, k_o is the free space wave vector, n_i is free space refractive index. Usually, the PGS is realized using a number of periodic unit cells of same inter-element spacing (P) and a pre-defined number of unit cells (N) to cover the full 360° phase range. Taking $\theta_i = 0^\circ$ and $n_i = 1$ then the direction of the reflected beam can be calculated using formula (2).

$$\theta_r = \arcsin\left(\frac{\lambda_o}{2\pi}\frac{\Delta\varphi}{\Delta x}\right) = \arcsin\left(\frac{\lambda_o}{2\pi}\frac{2\pi}{NP}\right).$$
$$\Rightarrow \theta_r = \arcsin\left(\frac{\lambda_o}{NP}\right) \quad (2)$$

In this way, the incident EM wave at a certain frequency can be reflected/steered to a predefined angle based on the design parameters (i.e. N and P) of the PGS.

In this paper the unit cell used to realize the 1D and 2D phase gradient dielectric perforated reflective surfaces is all dielectric unit cell as shown in Fig. 1(a). The unit cell has four air-filled drilled holes and the diameter of those holes determines the reflection phase value as the effective permittivity of the dielectric substrate is altered after drilling the holes. With such super cell configuration, the phase change (phase jumps) along the interface is about 72° ($2\pi/5 = 72^\circ$). All unit cells are simulated under the same boundary conditions using 3D high-frequency full-wave EM simulator, where the unit cell is surrounded by Master-Slave boundary conditions and terminated to a floquet port and backed by a solid perfect electrical conductor (PEC) ground. Then the floquet port is embedded to the top surface of the unit cell. The reflection phase characteristics of the five unit cells are then computed and presented in Fig. 1(b) and at 70 GHz there is a constant phase difference of about 70° between the reflected waves from those unit cells based on the diameter of the drilled air holes. Moreover, full wave simulations are performed to compute the backscattered E-field distribution of the individual unit cells (located at $z =$ 0) composing the super unit cell under normal incidence and the results are plotted in Fig. 1(c). As can be seen, each unit cell provides a specific discrete phase shift as the radius of the unit cells increased gradually from 0.21 to 0.3 mm.

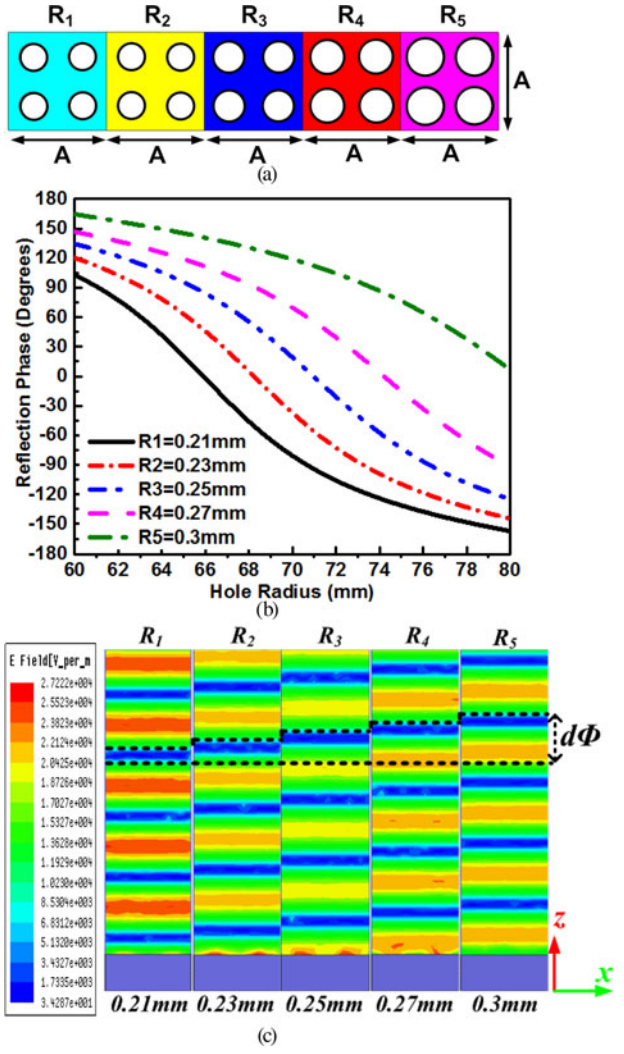

Fig. 1. The layout and the reflection characteristics of the unit cell used to realize the 1D and 2D phase gradient dielectric surfaces. (a) Super unit cell consists of five sub-unit cells: $A = 1.5$ mm, $R_1 = 0.21$ mm, $R_2 = 0.23$ mm, $R_3 = 0.25$ mm, $R_4 = 0.27$ mm, $R_5 = 0.3$ mm, $h = 1.27$ mm, $\varepsilon_r = 10.2$. (b) Reflection phase versus frequency curve of the unit cells. (c) E-field distribution of the super unit cell where $d\Phi$ is the phase change.

III. 1D AND 2D PGSs DESIGN

Using the super cell in Fig. 1(a), building blocks of 1 × 5 and 2 × 10 super cells and occupied an area of 7.5 × 7.5 and 15 × 15 mm² are designed as shown in Figs 2(a) and 2(b). The design parameters of these dielectric PGSs are $P = 1.5$ mm and $N = 5$. The direction of the reflected beam under normal incidence can be calculated using equation (2) and it is found that $\theta_r \approx 34.7^\circ$ at 70 GHz. A series of full-wave simulations are performed to compute the backscattered characteristics of the PGS in Figs 2(a) and 2(b) and the results are presented in Figs 2(c) and 2(d) with the backscattered pattern of their equivalent bare PEC surface in Figs 2(e) and 2(f) for comparison purposes. These results show that under normal incidence of EM-wave ($\theta_i = 0^\circ$), anomalous reflection is generated and the direction of the reflected beam is at about $\theta_r \approx 32.2^\circ$ ($\theta_r \neq \theta_i$) which is in good agreement with the predicted angles calculated by the generalized law of reflection (equation (2)) which is not the case for their equivalent bare PEC plates for which both the incident and reflected beams have equal angles ($\theta_r = \theta_i$) according to Snell's law of reflection. Another phase gradient reflective surface of different unit cell distribution is composed as shown in Fig. 3(a) and its computed backscattered RCS versus frequency under normal incidence is presented in Fig. 3(b). As can be seen, a clear reduction of more than 6 dBsm in the backscattered RCS is considered from about 69.1–78.5 GHz. The out-band and in-band 3D backscattered RCS field pattern (computed using CST Microwave Studio) of this surface is presented in Figs 4(a) and 4(b), respectively, which shows that anomalous reflection (at 70 GHz) is generated as two reflected beams in θ_r direction as confirmed by the 2D field distribution in Figs 4(c) and 4(d) which shows that the dielectric surface act as PEC surface at out band frequencies.

https://doi.org/10.1017/S1759078717001337 Published online by Cambridge University Press

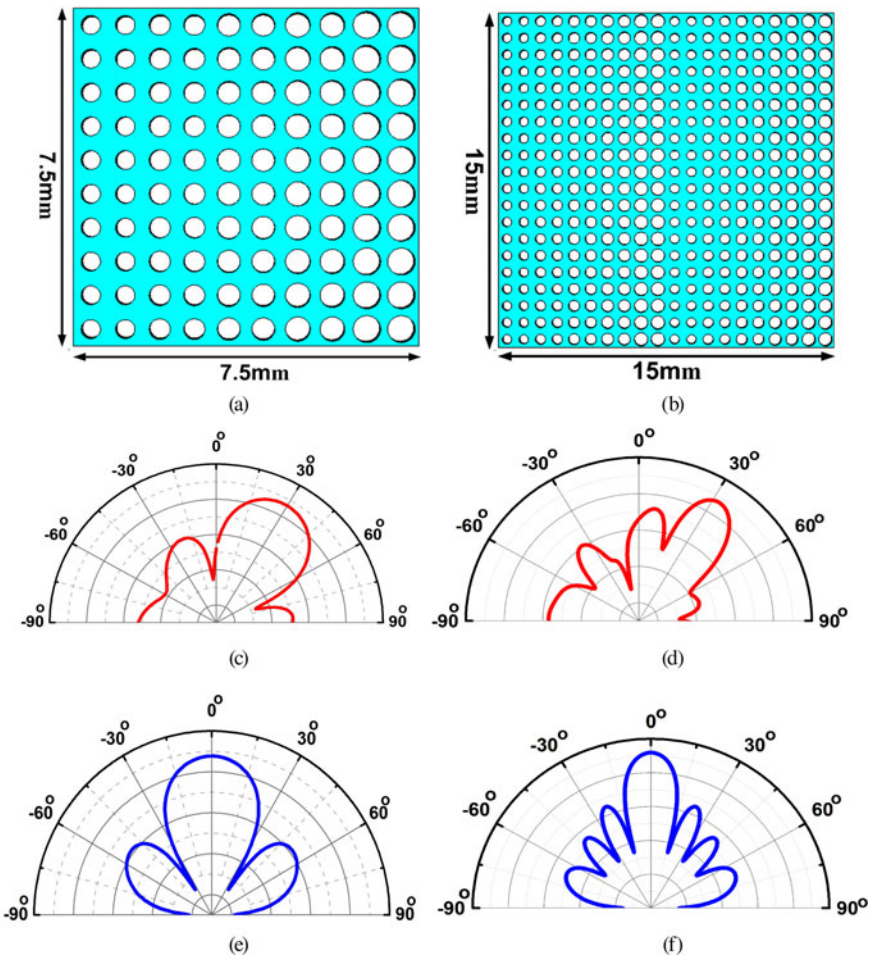

Fig. 2. The layout of the 1D PGS: (a) 7.5 mm × 7.5 mm and (b) 15 mm × 15 mm. Polar RCS patterns under normal incidence of a far-field plane wave: (c) 1D PGS in (a), (d) 1D PGS in (b), (e) Bare PEC plate: 7.5 mm × 7.5 mm. (f) Bare PEC plate: 15 mm × 15 mm.

In 2D PGS case there is a phase change (discontinuity) along both x- and y-axis, i.e. $\Delta\phi/\Delta x$ and $\Delta\phi/\Delta y$. In this case the reflected beam cannot be described by only one angle as in the case of the 1D PGS and two angles named θ_{r1} and θ_{r2} are required, where the angle θ_{r1} is the angle between the incident and reflected beam and θ_{r2} is the angle between x-axis and the projection of the reflected beam in xy-plane as can be seen in Fig. 5. Under normal incident of EM wave, θ_{r1} and θ_{r2} can be calculated as in equations (3) and (4). As can be seen in equations (3) and (4) there is more freedom in controlling the reflected beam in both azimuth and elevation planes.

$$\theta_{r1} = \arcsin\left[\frac{1}{k_o}\sqrt{(d\varphi/dx)^2 + (d\varphi/dy)^2}\right] = \arcsin\left[\frac{2\pi}{k_o} \times \sqrt{(1/N_x P_x)^2 + (1/N_y P_y)^2}\right], \quad (3)$$

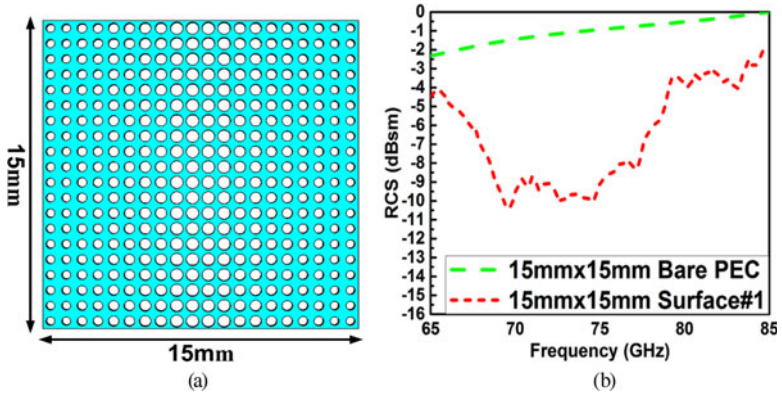

Fig. 3. The layout of the 1D phase gradient dielectric surfaces with its RCS reduction characteristics. (a) Surface #1: 15 mm × 15 mm. (b) RCS reduction curves.

https://doi.org/10.1017/S1759078717001337 Published online by Cambridge University Press

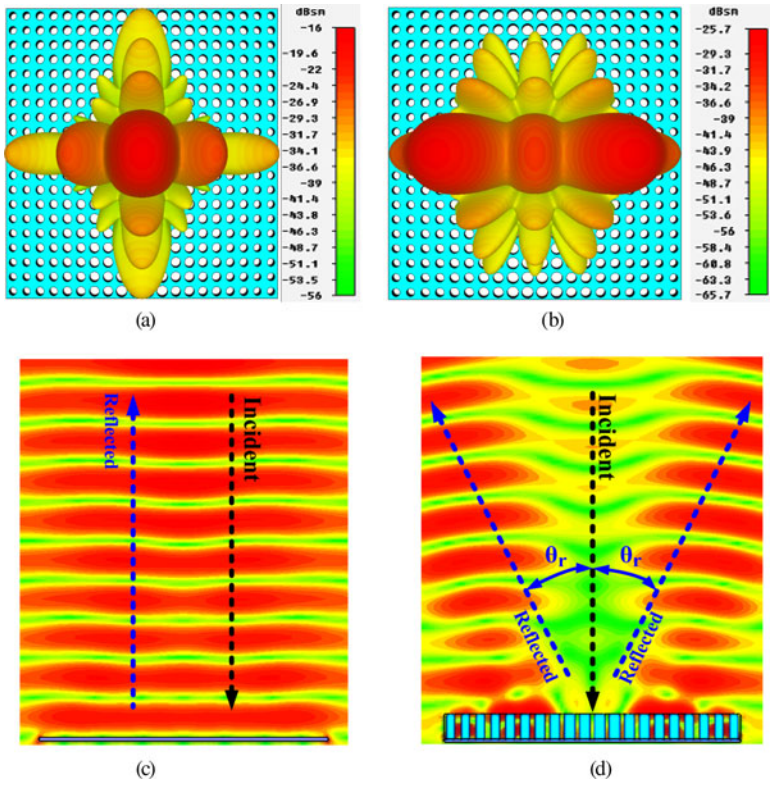

Fig. 4. The backscattered field distribution in front of the surfaces. The surface is placed in *xy*-plane symmetric with respect to the origin point (0, 0, 0). (a) Surface #1 at 85 GHz (out-band). (b) Surface #1 at 70 GHz (in-band). (c) 15 mm × 15 mm PEC Plate at 70 GHz. (d) Surface #1 at 70 GHz.

$$\theta_{r2} = \arctan(N_x P_x / N_y P_y). \quad (4)$$

The five-unit cells in Fig. 1(a) are used to form the 2D building blocks of 2D PGS of different unit cell distribution as shown in Fig. 6 with their unit cell distribution map. The layout of the designed 2D PGS is presented in Figs 7(a) and 7(b) where the main diagonal and distribution of the unit cells are different. The computed backscattered RCS under normal incidence for both surfaces is presented in Fig. 7(c) and both surfaces have a very close scattering characteristics and a clear reduction in the monostatic RCS is considered compared with its equivalent PEC plate. Moreover, the direction of the reflected beams is calculated using equations (3) and (4) where $\theta_{r1} = 53.8^\circ$ and $\theta_{r2} = 45^\circ$ and computed by full-wave simulations through CST microwave studio as shown in Fig. 7(d) and it is found to be $\theta_{r1} = 51.3^\circ$ and $\theta_{r2} = 45^\circ$.

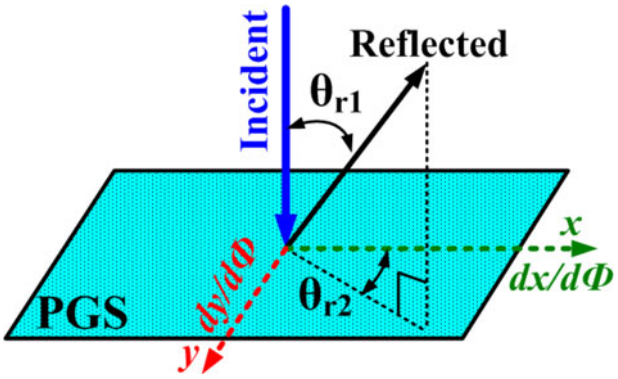

Fig. 5. Illustration of 2D phase gradient anomalous reflection angles.

IV. FABRICATION AND EXPERIMENTAL RESULTS

To further verify the presented designs, the 2D surface in Fig. 7(b) is fabricated using standard printed circuit board technology. The size of the fabricated square sample is 30 × 30 mm² and consists of 20 × 20 unit cells as shown in Fig. 8(a) with its equivalent bare PEC in Fig. 8(b). All fabricated surfaces are etched on 1.27 mm RO6010 high-frequency laminate. The geometrical parameters of the fabricated surface are the same as those used in the numerical simulations in Section III. The fabricated samples are mounted inside a dielectric holder ($\varepsilon_r \approx 1$) for measurement in an anechoic chamber. A single pyramidal horn antenna is used in the measurement which is fabricated using 1 mm thick copper sheet and connected to the measurement facilities via waveguide transition part as shown in Fig. 8. For reflectivity measurements [11] to be performed an Agilent N5245A network analyzer (calibrated using Agilent V11644A cal-kit) is used. The horn antenna is then connected directly to an Agilent millimeter wave VNA extender via 50 mm long WR-12 → WR-15 (and WR-12 → WR-10) waveguide transition parts. Microwave pyramidal absorbers are used to reduce the reflections from the unwanted surroundings. The horn antenna is placed as high as the fabricated sample in the experiment with enough distance (R) between them to avoid the near field effect. The distance R

https://doi.org/10.1017/S1759078717001337 Published online by Cambridge University Press

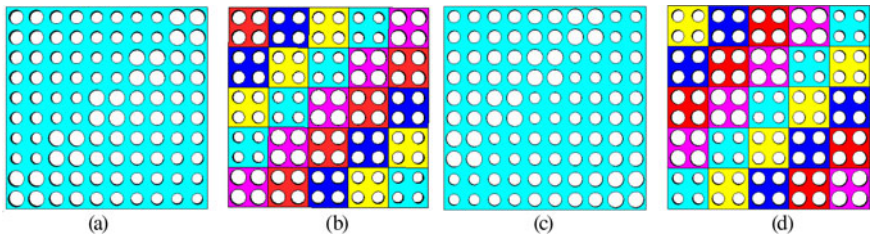

Fig. 6. The configuration of the 2D super unit cell of size 7.5 mm × 7.5 mm in which the main diagonal has unit cells have $R = 0.3$ mm, and $R = 0.21$ mm for (a) and (c), respectively. (b) and (d) shows the unit cell distribution map.

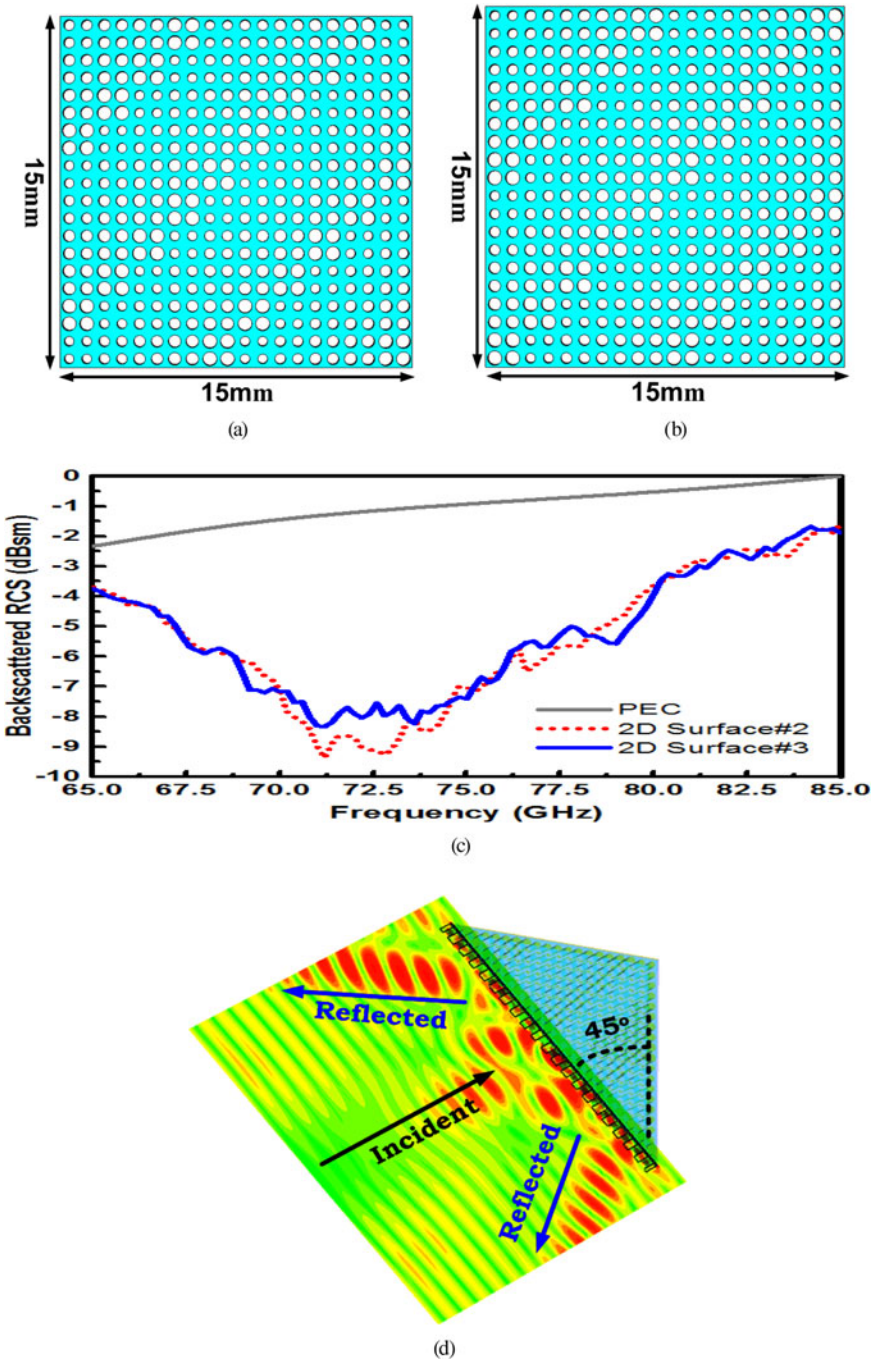

Fig. 7. (a) Surface #2: 15 mm × 15 mm. (b) Surface #3: 15 mm × 15 mm. (c) Monostatic RCS characteristics under normal incidence. (d) The backscattered field distribution in front of the surfaces at 70 GHz.

https://doi.org/10.1017/S1759078717001337 Published online by Cambridge University Press

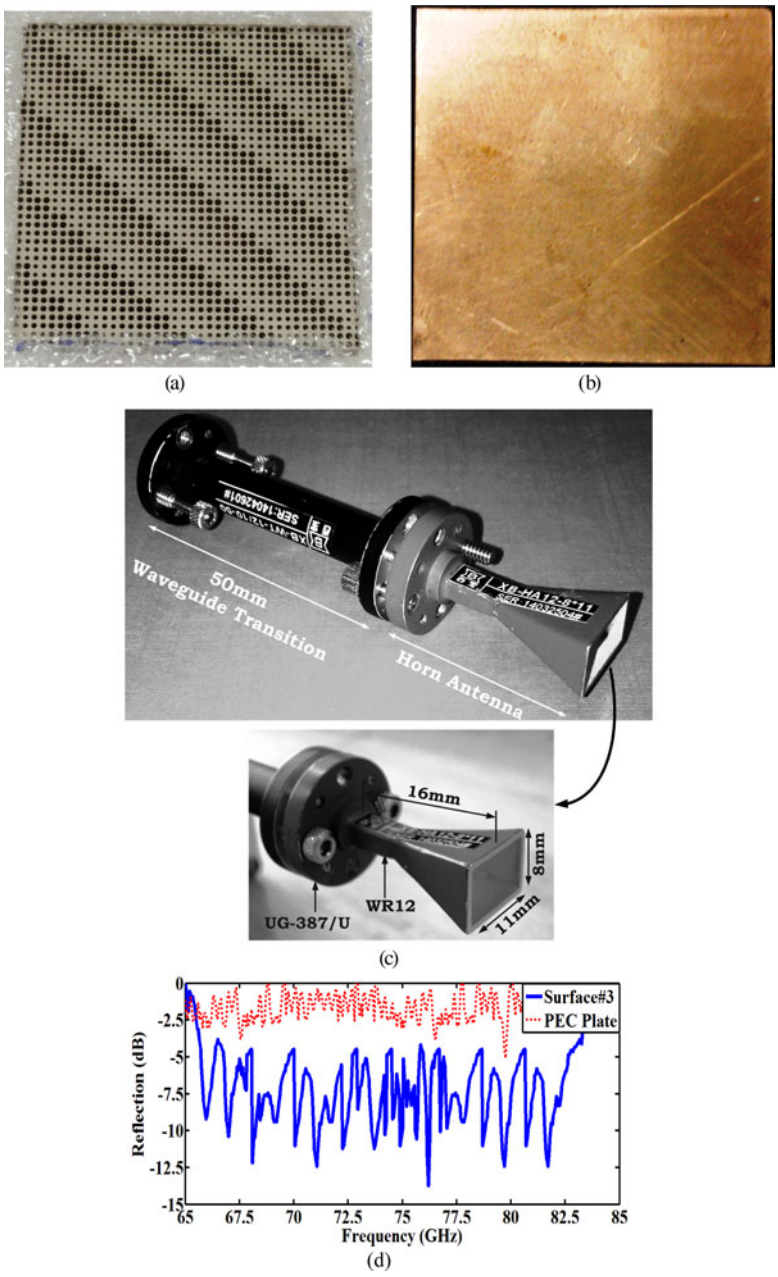

Fig. 8. Photograph of the fabricated (a) surface #3 and (b) the equivalent bare PEC plate. (c) Horn antenna and waveguide extension used in the measurements. (d) Measured reflectance versus frequency from the dielectric surface and bare PEC plate under normal incidence.

is calculated using a very well-known far-field region formula $R > 2D^2/\lambda$ in [12] where D is the surface aperture size and lambda is the free space wavelength. The results of the reflectivity measurements are presented in Fig. 8(c) and show a clear reduction in the backscattered (reflected) power in the boresight direction. This reduction is because the incident power is redirected away from the source (horn antenna), in other words, away from the boresight direction and not reflected back to the direction where it has come from. The measured results in Fig. 8(d) are a little deviated from the simulated results, this deviation can be attributed to number of factors such as: (i) the misalignments between the PGS under test and the horn antenna used in the measurements, (ii) in simulation the PGS is excited with a far-field plane wave which is not the case in the measurements where horn antenna is used as EM-wave radiator, and (iii) the manufacturing error of the PGS.

V. CONCLUSION

In summary, in this paper, the design of all dielectric 1D and 2D PGSs that can efficiently control the reflected waves and reflect the incident EM-wave to a pre-defined reflection angle is presented at millimeter wave frequencies. By adjusting the dimensions of the air-filled drilled holes inside the dielectric unit cell, it is shown that it is possible to obtain a constant phase gradient across the surface aperture. The possibility of using the presented surfaces to reduce the monostatic RCS in the boresight direction is investigated both numerically and experimentally.

https://doi.org/10.1017/S1759078717001337 Published online by Cambridge University Press

ACKNOWLEDGEMENT

The authors would like to thank the anonymous reviewers for their helpful and constructive comments that greatly contributed to improving the quality of the final version of this article. They also would like to thank the Editors for their generous comments and support during the review process. The authors also would like to thank Professor Z. Q. Kuai and Mr. H. T. Yi for the help with fabrication of the horn antennas and the presented surfaces.

REFERENCES

[1] Yu, N.F. et al.: Light propagation with phase discontinuities: generalized laws of reflection and refraction. Science, **334** (2011), 333–337.

[2] Sun, S.L.; He, Q.; Xiao, S.Y.; Xu, Q.; Li, X.; Zhou, L.: Gradient-index meta-surfaces as a bridge linking propagating waves and surface waves. Nat. Mat., **11** (2012), 426.

[3] Li, H.; Wang, G.; Xu, H.; Cai, T.; Liang, J.: X-Band phase-gradient metasurface for high-gain lens antenna application. IEEE Trans. Antennas Propag., **63** (2015), 5144–5149.

[4] Chen, W.; Balanis, C.A.; Birtcher, C.: Checkerboard EBG surfaces for wideband radar cross section reduction. IEEE Trans. Antennas Propag., **63** (2015), 2636–2645.

[5] Saeidi, C.; van der Weide, D.: Wideband plasmonic focusing metasurfaces. Appl. Phys. Lett., **105** (2014), 053107.

[6] Cai, T. et al.: Ultra-thin polarization beam splitter using 2-D transmissive phase gradient metasurface. IEEE Trans. Antennas Propag., **63** (2015), 5629–5636.

[7] Wang, J. et al.: Manipulating The Reflection Of Electromagnetic Waves Using Reflective Metasurfaces, in Proc. of 2014 3rd Asia-Pacific Conf. on Antennas and Propagation, Harbin, China, 2014.

[8] Hwang, R.-B.; Tsai, Y.-L.: Reflection characteristics of a composite planar AMC surface. AIP Advances, **2** (2012), 012128.

[9] Chen, H.Y. et al.: High-efficiency Anomalous Reflection Characteristics of an Ultra-thin Gradient Meta-surface Based on SRRs, in Progress In Electromagnetics Research Symp Proc., Guangzhou, China, 2014.

[10] Jia, N.; Chen, K.; Zhu, B.; Feng, Y.: Electromagnetic Wave Deflection And Backward Scattering Reduction By Flat Meta-Surfaces, in Proc.of 2014 3rd Asia-Pacific Conf. on Antennas and Propagation, Harbin, 2014, 1002–1005.

[11] Yang, X.M.; Jiang, G.L.; Liu, X.G.; Weng, C.X.: Suppression of Specular Reflections by Metasurface with Engineered Nonuniform Distribution of Reflection Phase, in Hindawi Int. Journal of Antennas and Propagation, Article ID 560403, January 2015.

[12] Balanis, C.A.: Antenna Theory, Analysis, and Design, 2nd ed., John Wiley and Sons, New York, 1997.

Mustafa K. Taher Al-Nuaimi was born in Iraq in 1980 and received the B.Sc. degree and the M.Sc. degree in 2003 and 2006, respectively, both in Communication Engineering. He received Ph.D. degree in Electromagnetic Field and Microwave Technology from Southeast University (SEU), Nanjing, China, in 2016. He is currently a Postdoctoral Research Fellow and member of the State Key Laboratory of Millimeter Waves of Southeast University in Nanjing, China. His current research interests include lens antennas, reflectarrays, metasurface, electromagnetic wave manipulation and radar cross section reduction. Dr. M. K. T. Al-Nuaimi is recipient of China Council Doctoral scholarship, Nanjing, China in 2011. In 2008 he received the Highlight in Microtechnology Scholarship, Nuchatel University, Switzerland. Dr. M. K. T. Al-Nuaimi is the recipient of the Best Student Paper Award at the 3rd Asia-Pacific Conference on Antennas and Propagation (APCAP2014) in Harbin, China, 2014. He is also the recipient of the Best Student Paper Award at the 2016 IEEE International Workshop on Electromagnetics (iWEM2016), Nanjing, China.

Wei Hong received the B.S. degree from the University of Information Engineering, Zhengzhou, China, in 1982, and the M.S. and Ph.D. degrees from Southeast University, Nanjing, China, in 1985 and 1988, respectively, all in radio engineering. Since 1988, he has been with the State Key Laboratory of Millimeter Waves and serves for the director of the lab since 2003, and is currently a professor and the dean of the School of Information Science and Engineering, Southeast University. In 1993, 1995, 1996, 1997 and 1998, he was a short-term Visiting Scholar with the University of California at Berkeley and at Santa Cruz, respectively. He has been engaged in numerical methods for electromagnetic problems, millimeter wave theory and technology, antennas, RF technology for wireless communications etc. He has authored and co-authored over 300 technical publications with over 9000 citations, and authored two books. He twice awarded the National Natural Prizes, thrice awarded the first-class Science and Technology Progress Prizes issued by the Ministry of Education of China and Jiangsu Province Government etc. Besides, he also received the Foundations for China Distinguished Young Investigators and for "Innovation Group" issued by NSF of China. Dr. Hong is a Fellow of IEEE, Fellow of CIE, the vice presidents of the CIE Microwave Society and Antenna Society, the Chair of the IEEE MTT-S/AP-S/EMC-S Joint Nanjing Chapter, and was an elected IEEE MTT-S AdCom Member during 2014–2016. He served as the Associate Editor of the IEEE Trans. On MTT from 2007 to 2010, one of the Guest editors for the 5G special issue of IEEE Trans. on AP in 2017.

Xiqi Gao received the Ph.D. degree in electrical engineering from Southeast University, Nanjing, China, in 1997. He joined the Department of Radio Engineering, Southeast University, in April 1992. Since May 2001, he has been a professor of information systems and communications. From September 1999 to August 2000, he was a visiting scholar at Massachusetts Institute of Technology, Cambridge, and Boston University, Boston, MA. From August 2007 to July 2008, he visited the Darmstadt University of Technology, Darmstadt, Germany, as a Humboldt scholar. His current research interests include broadband multicarrier communications, MIMO wireless communications, channel estimation and turbo equalization, and multirate signal processing for wireless communications. From 2007 to 2012, he served as an Editor for the IEEE Transactions on Wireless Communications. From 2009 to 2013, he served as an Associate Editor for the IEEE Transactions on Signal Processing. He now serves as an Editor for the IEEE Transactions on Communications. Dr. Gao received the Science and Technology Awards of the State Education Ministry of China in 1998, 2006 and 2009, the National Technological Invention Award of China in 2011, and the 2011 IEEE Communications Society Stephen O. Rice Prize Paper Award in the field of communications theory.